

First principles study of the water adsorption on anatase (101) as a function of the coverage.

Ruth Martinez-Casado,^{*,†,‡} Giuseppe Mallia,[¶] Nicholas M. Harrison,[¶] and Rubén Pérez^{§,||}

[†]*Univ Turin, Dipartimento Chim, IFM, I-10125 Turin, Italy*

[‡]*C.R.F. S.C.p.A Strada Torino 50, 10043 Orbassano (TO), Italy*

[¶]*Department of Chemistry, Imperial College London, South Kensington, London, SW7 2AZ, UK*

[§]*Departamento de Física Teórica de la Materia Condensada, Universidad Autónoma de Madrid, E-28049 Madrid, Spain*

^{||}*Condensed Matter Physics Center (IFIMAC), Universidad Autónoma de Madrid, Madrid 28049, Spain*

E-mail: ruthmcasado@gmail.com

Abstract

An understanding of the interaction of water with the anatase (101) surface is crucial for developing strategies to improve the efficiency of the photocatalytic reactions involved in solar water splitting. Despite a number of previous investigations, it is still not clear if water preferentially adsorbs in its molecular or dissociated form on anatase (101). With the aim of shedding some light on this controversial issue, we report the results of periodic screened-exchange density functional theory calculations of the dissociative, molecular and mixed adsorption modes on the anatase (101) surface at various coverages. Our calculations support the suggestion that surface adsorbed OH groups are present which has been made on the basis of recently measured X-ray photoelectron spectroscopy, temperature programmed desorption and scanning tunnelling microscopy data. It is also shown that the relative stability of water adsorption on anatase (101) can be understood in terms of a simple model based on the number and nature of the hydrogen bonds formed as well as the adsorbate-induced atomic displacements in the surface layers. These general conclusions are found to be insensitive to the specific choice of approximation for electronic exchange and correlation within density functional theory. The simple model of water-anatase interactions presented here may be of wider validity in determining the geometry of water-oxide interfaces.

1 Introduction

TiO₂, as a wide band gap semiconductor, has many applications including, as an heterogeneous catalyst,¹ as the transport medium in dye-sensitised solar cells,² and as the catalysis in photoelectrochemical water splitting for the carbon free production of hydrogen.^{3,4} An understanding of water chemistry on TiO₂ is crucial to facilitate the design of more efficient systems. Water can adsorb on TiO₂ surfaces molecularly or dissociatively. Molecular adsorption (in its most energetically favourable configuration) involves the direct interaction of the oxygen atom of the molecule with the fivefold-coordinated titanium, Ti_{5c}, of the surface.

In the dissociative adsorption mode an hydrogen atom is transferred from the molecule to a nearby under-coordinated surface oxygen ion. Two surface hydroxyls are thus formed: the hydroxyl bonded to the surface Ti_{5c} , which is generally called terminal hydroxyl, OH_{th} , and that resulting from the detached hydrogen and nearby oxygen ion; the bridging hydroxyl, OH_{bh} .

Rutile is the most stable bulk phase of titania; however, anatase nanoparticles are the most active photocatalyst.^{5,6} The (101) surface is the most stable anatase surface and represents a significant portion of the exposed surface area in nanostructures.⁷⁻⁹ Despite significant research effort in this area, there is still some controversy over the nature of the first water monolayer on the anatase (101) surface and in particular over whether there is molecular or dissociative adsorption. Until a few years ago, X-ray photoelectron spectroscopy (XPS),¹⁰ temperature programmed desorption (TPD),¹⁰ and scanning tunneling microscope (STM)¹¹ experiments seemed to agree with density functional theory (DFT) calculations¹²⁻¹⁴ that only molecular adsorption occurs on the pristine anatase (101) surface. A recent high-resolution XPS study,¹⁵ however, reported the presence of OH groups at the surface and challenged the accepted model of the interface. Subsequent DFT^{16,17} and force field¹⁸ studies support this result predicting mixed molecular and dissociative adsorption on anatase (101) for coverages from half to one monolayer. In recent calculations the detailed energetics of adsorption have been computed using hybrid exchange density functional theory, PBE0, but without an analysis of the structure at the full monolayer coverage that is observed or a discussion of the number and nature of the hydrogen bonds present at the interface.¹⁶ It is now well established that consideration of inter-molecular interactions is essential for an understanding of the water-oxide interface structure.^{19,20} The importance of the quantum nature of the hydrogen bonds for interface structure and properties has also been explored.^{21,22}

The purpose of the present work is to shed some light on the nature of the water-water and water-anatase(101) interactions that determine the interfacial structure. To achieve this, calculations are performed as a function of the coverage (defined as the ratio between

the number of adsorbed H₂O molecules and the number of surface Ti_{5c} sites). The adopted method is DFT using the screened hybrid exchange functional HSE;²³ we also present results obtained with the gradient corrected PBE functional to determine the sensitivity of the conclusions to the approximate treatment of electronic exchange and correlation. The results and discussion presented here lead to the idea that water adsorption on anatase (101) can be described by a simple model that supports the suggestion that OH groups are present at the surface. This model emphasises the importance of the number and nature of the adsorbate-adsorbate and adsorbate-surface hydrogen bonds for determining the structure of the interface.

The HSE functional has the advantage that in general it describes surface adsorption energetics and structures somewhat better than the PBE functional, partially corrects for electronic self-interaction and so yields qualitatively correct fundamental band gaps in wide band gap transition metal oxides and retains a reasonable description of semiconductors and metals.^{24,25}

2 Computational details

All calculations have been performed using the CRYSTAL14 software package,²⁶ based on the expansion of the crystalline orbitals as a linear combination of a local basis set (BS) consisting of atom-centered Gaussian orbitals with *s*, *p*, or *d* symmetry. The choice of the BS is the main numerical approximation in these calculations; in order to approach the BS limit, a hierarchy of all-electron basis sets, labeled as BS1, BS2 and BS3 (see Table 1), have been selected for O, Ti. The most complete basis set (BS3) has been used for the calculations.

The anatase structure belongs to the I4/amd tetragonal space group and the unit cell is defined by the lattice vectors *a* and *c* and the oxygen internal coordinate *u*. The primitive cell contains two atoms in the asymmetric unit: a Ti ion at (0,0,0) and an O ion at (0,0,*u*),

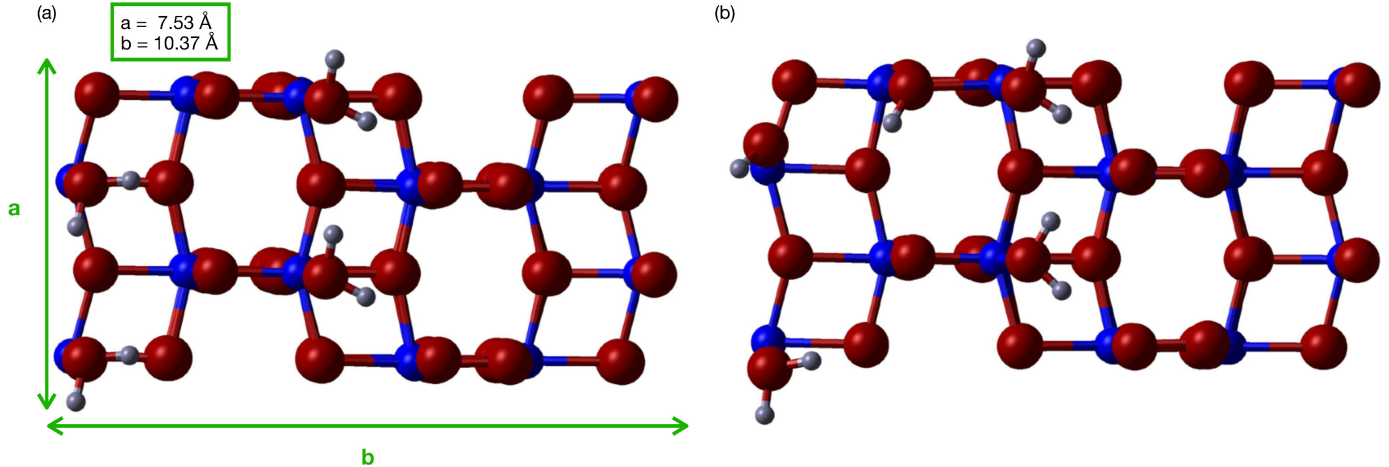


Figure 1: (Color online) Top view of the optimised structures resulting from the adsorption of water on anatase (101) at full monolayer coverage and for the cases: (a) molecular adsorption by using the HSE functional, (b) mixed adsorption by using the HSE functional. Large (red), medium (blue), and small (grey) spheres correspond to oxygen, titanium, and hydrogen, respectively.

in fractional coordinates. Each Ti is octahedrally coordinated to six O ions. The TiO_6 octahedron is distorted, with the length of the two apical Ti- O_{ap} bonds slightly longer than the four equatorial, Ti- O_{eq} , bonds. The anatase TiO_6 octahedron shares four edges in adjacent pairs.

The surface is simulated by using a slab, which is periodic in two dimensions but finite in the third for which the boundary condition is that the wave function decays to zero at infinite distance from the surface. The slab is cut from the bulk crystal fully optimised with respect to lattice parameters and atomic coordinates. The slab consists of four TiO_2 trilayers with the in-plane periodicity given by a 1×2 supercell of the conventional surface cell. The surface unit cell dimensions are therefore: $10.48 \times 7.60 \text{ \AA}$ for PBE and $10.37 \times 7.53 \text{ \AA}$ for HSE (see Fig. 1).

Integration over reciprocal space was carried out on a symmetrised Monkhorst-Pack²⁷ with shrinking factor 4 for the 2D slab cell (and the shrinking factor was kept consistent for supercells). Matrix elements of the exchange and correlation potentials and the energy functional are integrated numerically on an atomcentered grid of points. The integration over radial and angular coordinates is performed using Gauss-Legendre and Lebedev schemes,

Table 1: All-electron basis set hierarchy for Ti, O, and H.

	Ti	O	H
BS1	8-6411d(1) (1s;4sp;1d)	8-611 (1s;3sp)	3-1p(1) (2s;1p)
BS2	8-6411d(11) (1s;4sp;2d)	8-611	3-1p(1)
BS3	8-6411d(11)	8-611(d1) (1s;3sp;1d)	3-1p(1)

respectively. A pruned grid consisting of 99 radial points and 5 sub-intervals with (146, 302, 590, 1454, 590) angular points has been used for all calculations (the XXLGRID option implemented in CRYSTAL14²⁶). This grid converges the integrated charge density to an accuracy of about 10^{-6} electrons per unit cell. These meshes converge the integrated charge density to an accuracy of about 10^{-6} electrons per unit cell. The Coulomb and exchange series are summed directly and truncated using overlap criteria with thresholds of [7,7,7,7,14].²⁸ The self-consistent field (SCF) iterations were considered to be converged when the change in energy was less than 10^{-7} Hartree per cell. Structural optimisation of internal coordinates was performed using the Broyden-Fletcher-Goldfarb-Shanno scheme. Convergence was determined from the root-mean-square (rms) and the absolute value of the largest component of the forces. The thresholds for the maximum and the rms forces (the maximum and the rms atomic displacements) have been set to 0.02 and 0.01 eV/Å (0.0009 and 0.0006 Å). Geometry optimisation was terminated when all four conditions were satisfied simultaneously.

3 Results and Discussion

3.1 Dilute limit

An initial model of isolated molecular adsorption is generated by placing a molecule above one of the four Ti_{5c} sites of the 2×1 surface supercell discussed above (Fig. 2 (a) and (d)). This corresponds to a coverage of $\Theta = 0.25ML$ with the minimum intermolecular spacing being 10.5Å at which distance inter-molecular interactions may be considered to

be negligible.¹⁶ Isolated dissociative adsorption is modelled by placing an OH_{th} group above the Ti_{5c} site, and a proton at a surface twofold coordinate O ion (O_{2c}), thereby generating a *bridging hydroxyl* group, OH_{bh}. There are two possible configurations for the OH_{th} which we denote as intrapair (Fig. 2 (b) and (e)) and interpair (Fig. 2 (c) and (d)) with the classification based on the H-bond acceptor involved in the H-bond interaction; the OH_{bh} or the lattice O respectively. Both molecular and dissociative adsorption modes are found to be locally stable during geometry optimisation.

A simple model based on the analysis of the hydrogen bonding can be used to rationalise the computed adsorption energies. The hydrogen bond in water involves an hydrogen (H), the oxygen (O1) to which is covalently bound, and a second hydrogen bond acceptor oxygen ion (O2). There are many classifications for the hydrogen bond in the literature, the one presented in Table 2 is the most commonly used and relates the strength of the bond to the O1-O2 and H-O2 distances.²⁹ An alternative method to assess the strength of hydrogen bonds has been recently presented, based on the proton-transfer coordinate ν , which is defined as $\nu = \text{distance}(\text{H-O1}) - \text{distance}(\text{H-O2})$; hydrogen bonds are not formed for $\nu \geq -1.25 \text{ \AA}$ ²¹. In the current context, both classification methods yield the same conclusion that for a $\text{distance}(\text{H-O2}) \geq 2.3 \text{ \AA}$, only weak hydrogen bonds are formed. The optimised structures computed in the HSE and PBE approximations are displayed in Fig. 2, together with the computed H-O2 distances. Molecular adsorption yields two medium strength hydrogen bonds in both approximations, while the dissociated water yields two weak bonds both for the intrapair and interpair configurations.

The presence of a medium strength hydrogen bond implies a contribution to the binding energy of around 0.17 eV (see Table 2); which is consistent with the fact that the computed energy of molecular adsorption (with two medium strength hydrogen bonds) is found to be more favourable by 0.30 eV than dissociative adsorption. This simple model is consistent with the calculated adsorption energies of each configuration in Table 3.

In order to understand how the adsorption structure affects the photochemistry of the

Table 2: Classification of hydrogen bonds.

	strong	medium	weak
bond energy (eV)	0.17-1.73	0.17-0.61	0.0-0.17
type	covalent	mostly electrostatic	electrostatic
distance (O1-O2) (Å)	2.2-2.5	2.5-3.2	3.2-4.0
distance (H-O2) (Å)	1.2-1.5	1.5-2.2	2.2-3.2
bond angle (degrees)	175-180	130-180	90-150

Table 3: Adsorption energies at the dilute limit for the HSE and PBE functionals. Previous plane wave (PW) results with the PBE functional have been added for comparison.

Method	Mol	Intra	E_{ads} (eV)	
			Inter	Diff (Inter-Mol)
LCAO-PBE	-0.71	-0.38	-0.34	0.37
LCAO-HSE	-0.84	-0.54	-0.49	0.35
PW-PBE ¹⁶	-0.69	-0.42	-0.37	0.32

surface, the projections of the density of states (DOS) on the eight outermost Ti_{5c} and O_{2c} atoms plus water are presented in Fig. 3 for the HSE functional. In the DOS of the anatase (101) surface (see Fig. 3 (a)) the valence band (VB) – below -5 eV – displays predominantly O-2p character, with some hybridization with Ti-3d orbitals; the conduction band (CB) – above 0eV – is derived mainly from Ti-3d atomic orbitals with some hybridization with O-2p orbitals.^{9,30,31} No significant changes can be seen when a water molecule is molecularly adsorbed on the surface (Fig. 3 (b)). On the other hand, the dissociately adsorbed molecules display significant hybridisation of the molecular O-2p states with those of the surface (Fig. 3 (c) and (d)). The results presented in this section are in agreement with previous DFT works,^{12,13,16} and generally support a model in which molecular adsorption dominates at the dilute limit.

3.2 Half monolayer coverage

In the molecular adsorption at half monolayer coverage ($\Theta = 0.5ML$), two water molecules are placed above two of the four Ti_{5c} sites of the (101) surface. There is a significant change in

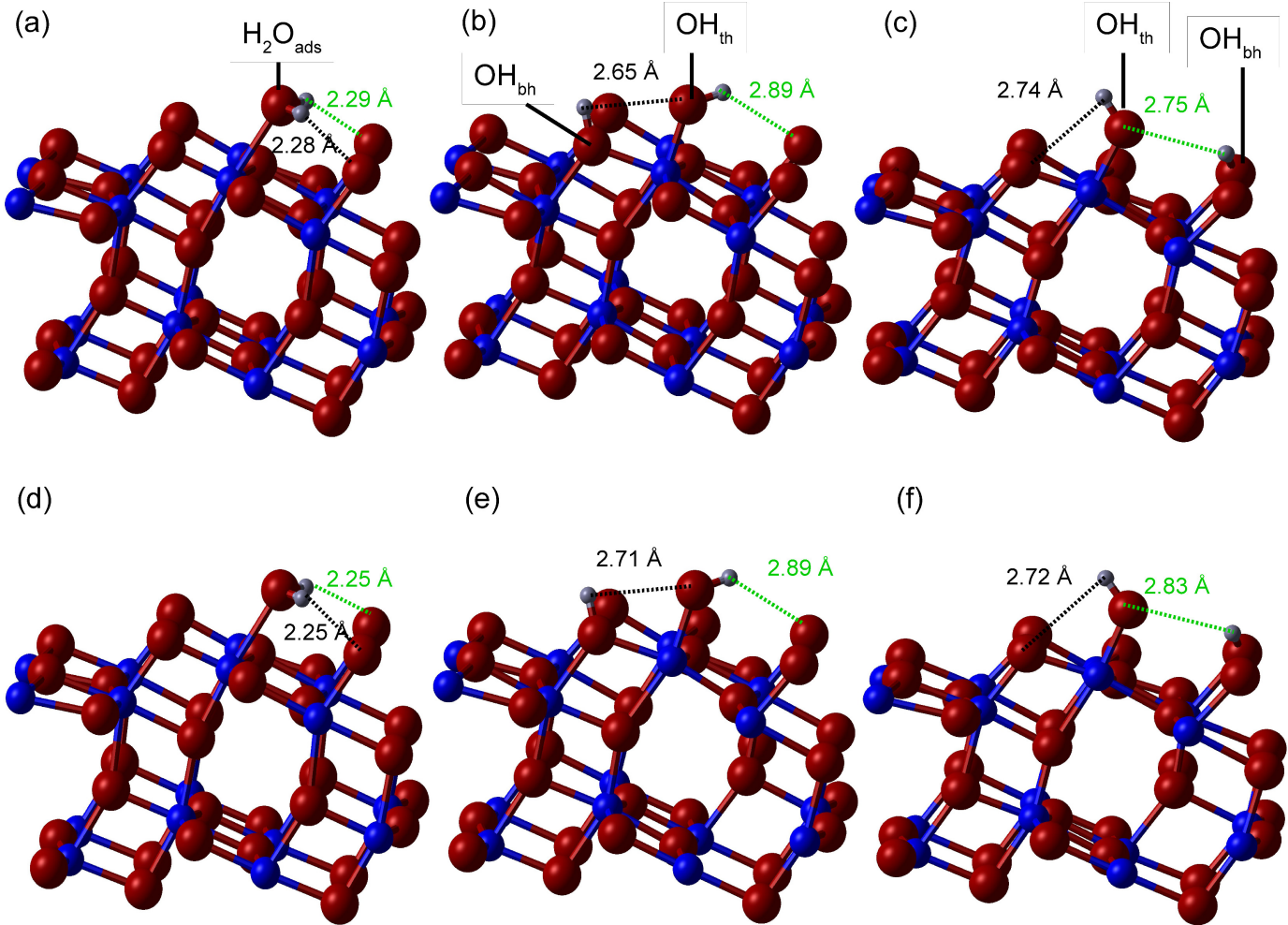


Figure 2: (Color online) Optimised structures and hydrogen bonds resulting from the adsorption of water on anatase (101) at the dilute limit for (a) HSE molecular, (b) HSE intramolecular dissociative, (c) HSE intermolecular dissociative, (d) PBE molecular, (e) PBE intramolecular dissociative, and (f) PBE intermolecular dissociative cases. O2-H distance is shown with dashed lines.

the optimised structure compared to the dilute case, as shown in Fig. 4, in calculations both HSE and PBE approximations. Water is a polar molecule with a partial negative charge at the oxygen end, while hydrogen atoms are partially positively charged. The hydrogen atoms of contiguous water molecules tend to repel each other favouring the formation of an hydrogen bond with the oxygen atom of the neighbouring water molecule. This behaviour, where three weak hydrogen bonds are formed, is reproduced by both considered functionals.

Concerning the mixed molecular-dissociated adsorption, we have presented here the most

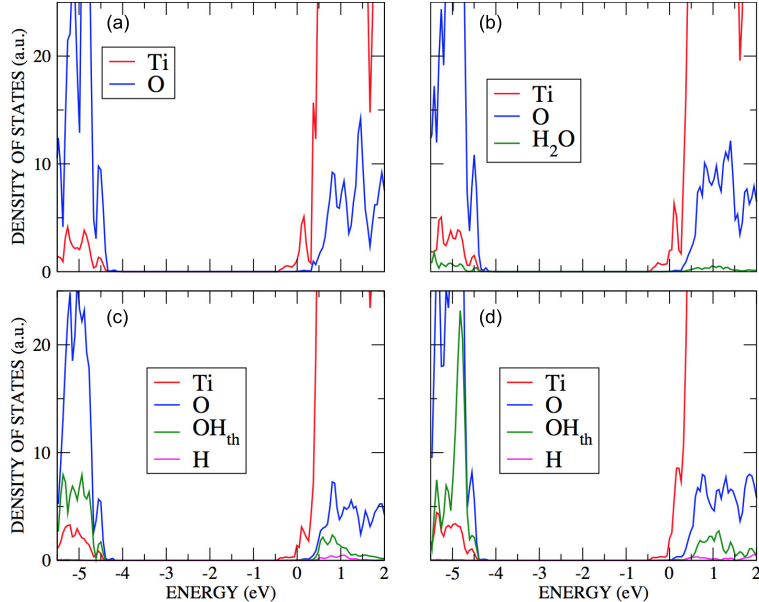


Figure 3: (Color online) DOS for anatase (101) at the dilute limit projected on the eight outermost Ti_{5c} and O_{2c} atoms plus water, when using the HSE functional, for the following cases: (a) clean surface, (b) molecular adsorption of water, (c) intramolecular dissociative adsorption of water, and (d) intermolecular dissociative adsorption of water.

energetically favourable configuration found which is consistent with that previously reported.^{15,16,32} In this configuration, shown in Fig. 4 (b) and (d), the OH_{th} group (at the Ti_{5c} site) and the OH_{bh} group form an hydrogen bond, ending up in three weak hydrogen bonds. The undissociated molecule and OH_{th} show hydrogen bonds with a neighbouring O_{2c} , while the H in OH_{bh} is linked to the O in OH_{th} . As a consequence, the same number of weak bonds are formed as in molecular adsorption. The optimised structures for the mixed adsorption are very similar for both functionals (Fig. 4). We have considered the detached hydrogen atom to form the OH_{bh} with the two possible O_{2c} sites allowed by our supercell, being the one presented in Fig. 4 the lower in energy

The DOS projected on the eight outermost Ti_{5c} and O_{2c} atoms plus water computed in the HSE approximation is presented in Fig. 5. In this mixed adsorption configuration, the O states from OH_{th} are strongly hybridised with the O states of the surface valence band – below -4 eV.

An analysis of the adsorption energies in Table 4 leads us to the conclusion that molecular

Table 4: Adsorption energies as a function of the coverage for the HSE and PBE functionals. Previous plane wave (PW) results with the PBE functional have been added for comparison.

Coverage (Θ)	Method	Mol	E_{ads} (eV)	
			Mixed	Diff (Mixed-Mol)
0.5	LCAO-PBE	-0.70	-0.63	0.07
0.5	LCAO-HSE	-0.81	-0.75	0.06
1.0	LCAO-PBE	-0.68	-0.65	0.02
1.0	LCAO-HSE	-0.77	-0.75	0.02
1.0	PW-PBE ¹⁶	-0.64	-0.58	0.06

and mixed adsorption modes have a very similar stability at half monolayer coverage; this is consistent with the number and type of bonds present. The DFT energy therefore suggest that the mixed adsorption is stable, something that is confirmed by the simple bonding model presented here. This result supports the conclusion that OH groups are present at the anatase (101) surface recently obtained from analysis of XPS data.¹⁵

3.3 Full monolayer coverage

Based on XPS measurements it has been suggested that at full monolayer coverage around 25% of the water molecules are dissociated.¹⁵ We explore this possibility by investigating a number of water-oxide interface configurations, one consisting of only molecular adsorption and several in which 25% of the molecules are dissociated (Fig. 6 (a) and (c)). The relaxed geometries of the molecular and lowest energy mixed configurations, among those consistent with the adopted 2D periodicity, found in the HSE and PBE approximations are displayed in Fig. 6.

For molecular adsorption the water molecules form two medium and four weak hydrogen bonds. In the mixed adsorption, two of the undissociated molecules form three medium hydrogen bonds, while the OH_{bh} group has a weak hydrogen bond to an O_{2c} . This overall bonding is insensitive to the choice of density functional.

The DOS for configurations at 1 ML coverage is presented in Fig. 7, there are no signif-

icant differences with respect to the 0.5 ML coverage. In both projected DOS plots (Fig. 5 and 7), the oxygen states of OH_{th} are strongly hybridized with the O states of anatase (101) at the top the valence band.

The adsorption energies presented in Table 3 suggest that at full coverage, as at half coverage, molecular and mixed adsorption modes have very similar energies (within 0.02 eV). This is consistent with the model suggested on the basis of XPS experiments.¹⁵ It is notable that a similar conclusion has been reached on the basis of STM data for water adsorbed at the rutile (110) surface.³³ The remarkably small change in the energy when one water molecule undergoes dissociation can be understood in terms of the h-bonding model. The loss of two of the three weak hydrogen bonds present in the molecular adsorption configuration is compensated by the formation of a medium strength h-bond between a remaining undissociated water molecule and a neighbouring O_{2c} .

4 Conclusions

In this study, the interaction of water with anatase (101) has been explored, as a function of the coverage, by analysing the geometrical and electronic properties. A detailed analysis of this system could help in the prediction of the structure and properties of other water-oxide interfaces. The model presented here is characterised by an interplay between chemisorption, hydrogen bonding and atomic displacements at the surface. Molecular, dissociative and mixed adsorption modes are studied at various coverage showing the mixed one to be more favourable as coverage increases. The projected density of states of the surface in contact with a mixture of adsorbed water molecules and adsorbed hydroxyls clarify the nature of the chemical bonds involved. Adsorbed water states on anatase (101) hybridise strongly with the O-2p states of the surface, this effect is not observed in other oxide surfaces as SnO_2 .³⁴ An analysis of the adsorption energies leads us to the conclusion that molecular and mixed dissociated adsorption have a very similar stability at half and full monolayer coverage. This

results is confirmed by the simple bonding model presented here. This result is consistent with the finding of OH groups at the anatase (101) surface recently reported by XPS.

Acknowledgement

We acknowledge financial support from the Fiat Research center, and a Juan de la Cierva contract (R.M.-C.). Computer time was provided by the Spanish Supercomputing Network (RES, Spain) at the Magerit Supercomputer (Madrid, Spain). This work made use of the high performance computing facilities of Imperial College London and, via our membership of the UK HPC Materials Chemistry Consortium, which is funded by EPSRC (EP/L000202).

References

- (1) Haruta, M.; Yamada, N.; Kobayashi, T.; Iijima, S. Gold catalysts prepared by coprecipitation for low-temperature oxidation of hydrogen and of carbon monoxide. *J. Catal.* **1989**, *115*, 301.
- (2) Graetzel, M. Photoelectrochemical cells. *Nature* **2001**, *414*, 338.
- (3) Fujishima, A.; Honda, K. Electrochemical Photolysis of Water at a Semiconductor Electrode. *Nature* **1972**, *238*, 37.
- (4) Listorti, A.; Durrant, J.; Barber, J. Structure and dynamics of liquid water on rutile TiO₂ (110). *Nat. Mater.* **2009**, *8*, 929.
- (5) Crossland, E. Mesoporous TiO₂ single crystals delivering enhanced mobility and optoelectronic device performance. *Nature* **2013**, *495*, 215.
- (6) Murdoch, M.; Waterhouse, G. I. N.; Nadeem, M. A.; Metson, J. B.; Keane, M. A.; Howe, R. F.; Llorca, J.; Idriss, H. The effect of gold loading and particle size on

- photocatalytic hydrogen production from ethanol over Au/TiO₂ nanoparticles. *Nature Chemistry* **2011**, *3*, 489, Article.
- (7) Labat, F.; Baranek, P.; Adamo, C. Structural and Electronic Properties of Selected Rutile and Anatase TiO₂ Surfaces: An ab Initio investigation. *J. Chem. Theory Comput.* **2008**, *4*, 341.
- (8) Lazzeri, M.; Vittadini, A.; Selloni, A. Structure and energetics of stoichiometric TiO₂ anatase surfaces. *Phys. Rev. B* **2001**, *63*, 155409.
- (9) Sanches, F.; Mallia, G.; Liborio, L.; Diebold, U.; Harrison, N. *Phys. Rev. B* **2014**, *89*, 245309.
- (10) Herman, G. S.; Dohnálek, Z.; Ruzycki, N.; Diebold, U. Experimental investigation of the interaction of water and methanol with anatase TiO₂ (101). *J. Phys. Chem. B* **2003**, *107*, 2788.
- (11) He, Y.; Tilocca, A.; Dulub, O.; Selloni, A.; Diebold, U. Local ordering and electronic signatures of submonolayer water on anatase TiO₂ (101). *Nat. Mater.* **2009**, *8*, 585.
- (12) Vittadini, A.; Selloni, A.; Rotzinger, F. P.; Graetzel, M. Structure and Energetics of Water Adsorbed at TiO₂ Anatase (101) and (00) Surfaces. *Phys. Rev. Lett.* **1998**, *81*, 2954.
- (13) Zhao, Z.; Li, Z.; Zou, Z. Understanding the interaction of water with anatase TiO₂ (101) surface from density functional theory calculations. *Phys. Lett. A* **2011**, *375*, 2939.
- (14) Sun, C.; Liu, L.; Selloni, A.; Lu, G. Q.; Smith, S. Titania-water interactions: a review of theoretical studies. *J. Mat. Chem.* **2010**, *20*, 10319.
- (15) Walle, L.; Borg, A.; Johansson, E.; Plogmaker, S.; Rensmo, H.; Uvdal, P.; Sandell, A. Mixed Dissociative and Molecular Water Adsorption on Anatase TiO₂ (101). *J. Phys. Chem. C* **2011**, *115*, 9545.

- (16) Patrick, C. E.; Giustino, F. Structure of a Water Monolayer on the Anatase TiO₂ (101) Surface. *Phys. Rev. Appl.* **2014**, *2*, 014001.
- (17) Deaka, P.; Kullgrenb, J.; Aradia, B.; Frauenheima, T.; Kavanc, L. Water splitting and the band edge positions of TiO₂. *Electrochimica Acta* **2016**, *199*, 27.
- (18) Raju, M.; Kim, S.-Y.; van Duin, A. C. T.; Fichthorn, K. A. ReaxFF Reactive Force Field Study of the Dissociation of Water on Titania Surfaces. *J. Phys. Chem. C* **2013**, *117*, 10558.
- (19) Lindan, P.; Harrison, N.; Holender, J.; Gillan, M. First-principles molecular dynamics simulation of water dissociation on TiO₂ (110). *Chemical Physics Letters* **1996**, *261*, 246 – 252.
- (20) Lindan, P. J. D.; Harrison, N. M.; Gillan, M. J. Mixed Dissociative and Molecular Adsorption of Water on the Rutile (110) Surface. *Phys. Rev. Lett.* **1998**, *80*, 762–765.
- (21) Ceriottia, M.; Cuny, J.; Parrinello, M.; Manolopoulos, D. E. Nuclear quantum effects and hydrogen bond fluctuations in water. *PNAS* **2013**, *110*, 15591.
- (22) Li, X.-Z.; Walker, B.; Michaelides, A. Quantum nature of the hydrogen bond. *PNAS* **2011**, *108*, 6369.
- (23) Krukau, A. V.; Vydrov, O. A.; Izmaylov, A. F.; Scuseria, G. E. Influence of the exchange screening parameter on the performance of screened hybrid functionals. *The Journal of Chemical Physics* **2006**, *125*, 224106.
- (24) Janesko, B. G.; Henderson, T. M.; Scuseria, G. E. Screened hybrid density functionals for solid-state chemistry and physics. *Phys. Chem. Chem. Phys.* **2009**, *11*, 443.
- (25) Pernot, P.; Civalleri, B.; Presti, D.; Savin, A. Prediction Uncertainty of Density Functional Approximations for Properties of Crystals with Cubic Symmetry. *J. Phys. Chem. A* **2015**, *119*, 5288–5304.

- (26) Dovesi, R.; Orlando, R.; Erba, A.; Zicovich-Wilson, C. M.; Civalleri, B.; Casassa, S.; Maschio, L.; Ferrabone, M.; Pierre, M. D. L.; D'Arco, P. et al. CRYSTAL14: A program for the ab initio investigation of crystalline solids. *Int. J. Quantum Chem.* **2014**, *114*, 1287.
- (27) Monkhorst, H. J.; Pack, J. D. Special points for Brillouin-zone integrations. *Phys. Rev. B* **1976**, *13*, 5188–5192.
- (28) Pisani, C.; Dovesi, R.; Roetti, C. *Hartree-Fock ab initio Treatment of Crystalline Systems*; Springer, 1988.
- (29) Desiraju, G.; Steiner, T. *The weak hydrogen bond in structural chemistry and biology*; Oxford University Press, 1999.
- (30) Casado, R. M.; Todorović, M.; Mallia, G.; Harrison, N.; Pérez, R. First principles calculations on defective (101) anatase surface: influence of basis sets and exchange functionals. *submitted to J. Phys. Chem. C* **2017**,
- (31) Stetsovych, O.; Todorović, M.; Shimizu, T. K.; Moreno, C.; Ryan, J. W.; León, C. P.; Sagisaka, K.; Palomares, E.; Matolín, V.; Fujita, D. et al. Atomic species identification at the (101) anatase surface by simultaneous scanning tunnelling and atomic force microscopy. *Nat. Comm.* **2015**, *6*, 7265.
- (32) Aschauer, U.; He, Y.; Cheng, H.; Li, S.-C.; Diebold, U.; Selloni, A. Influence of Sub-surface Defects on the Surface Reactivity of TiO₂: Water on Anatase (101). *J. Phys. Chem. C* **2010**, *114*, 1278.
- (33) Wang, Z.; Wang, Y.; Mu, R.; Yoon, Y.; Dahal, A.; Schenter, G. K.; Glezakou, V.; Rousseau, R.; Lyubinetsky, I.; Dohnálek, Z. Probing equilibrium of molecular and de-protonated water on TiO₂(110). *PNAS* **2017**, *114*, 1801.

- (34) Patel, M.; Sanches, F.; Mallia, G.; Harrison, N. A quantum mechanical study of water adsorption on the (110) surfaces of rutile SnO₂ and TiO₂: investigating the effects of intermolecular interactions using hybrid-exchange density functional theory. *Phys. Chem. Chem. Phys.* **2014**, *16*, 21002.

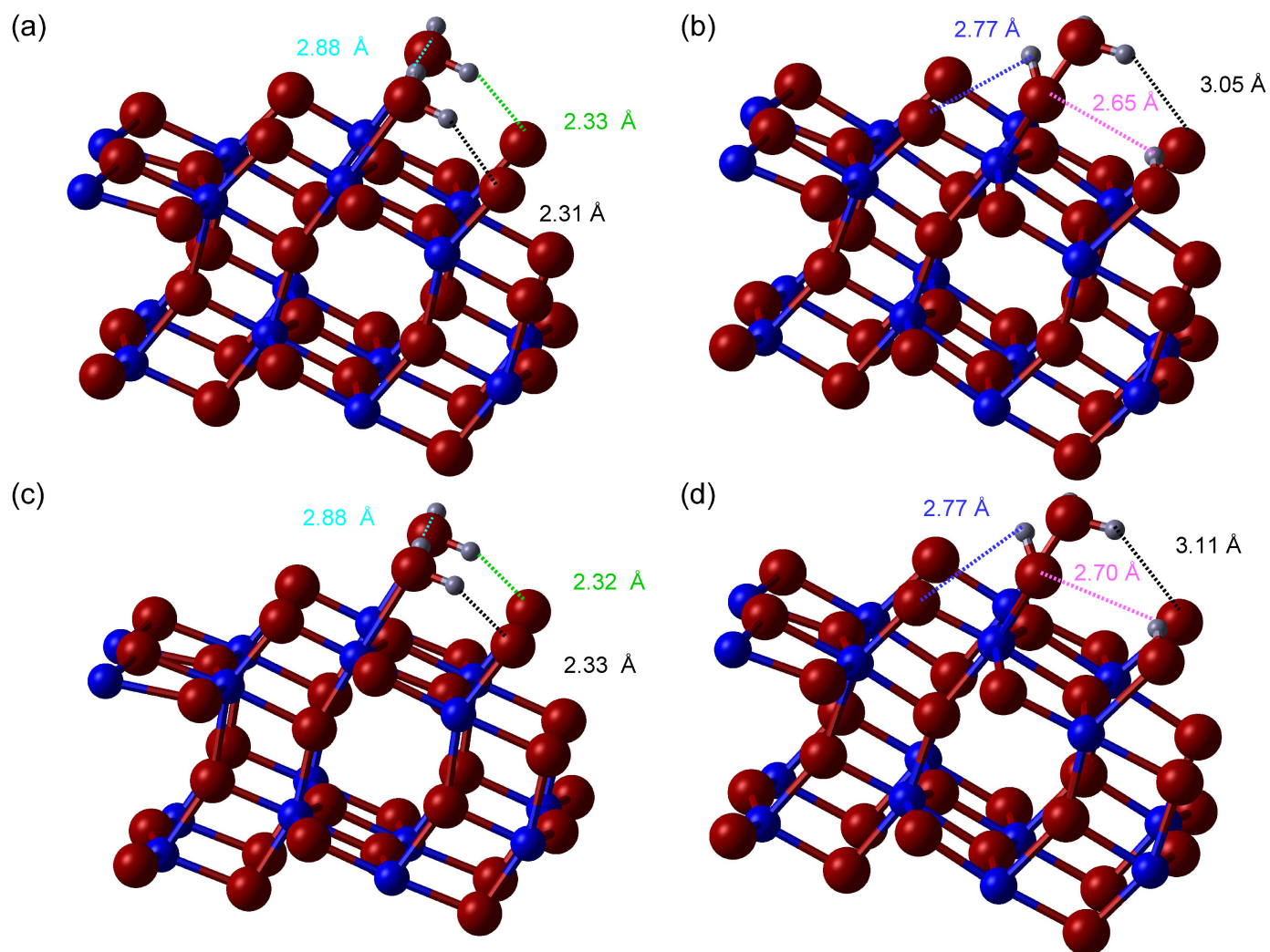


Figure 4: (Color online) Optimised structures and hydrogen bonds resulting from the adsorption of water on anatase (101) at half monolayer coverage and the cases: (a) HSE-molecular, (b) HSE-mixed, (c) PBE-molecular, and (d) PBE-mixed. O2-H distance is shown with dashed lines.

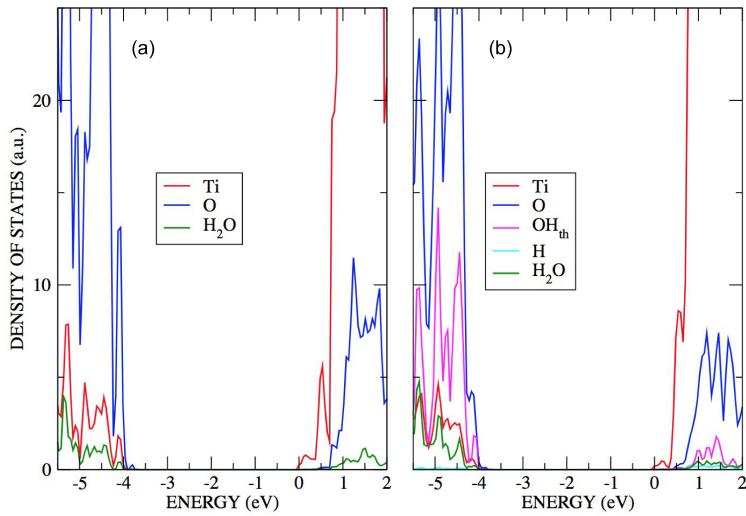


Figure 5: (Color online) DOS for anatase (101) at half monolayer coverage projected on the eight outermost Ti_{5c} and O_{2c} atoms plus water and using the HSE functional for the cases: (a) molecular adsorption of water, and (b) mixed adsorption of water.

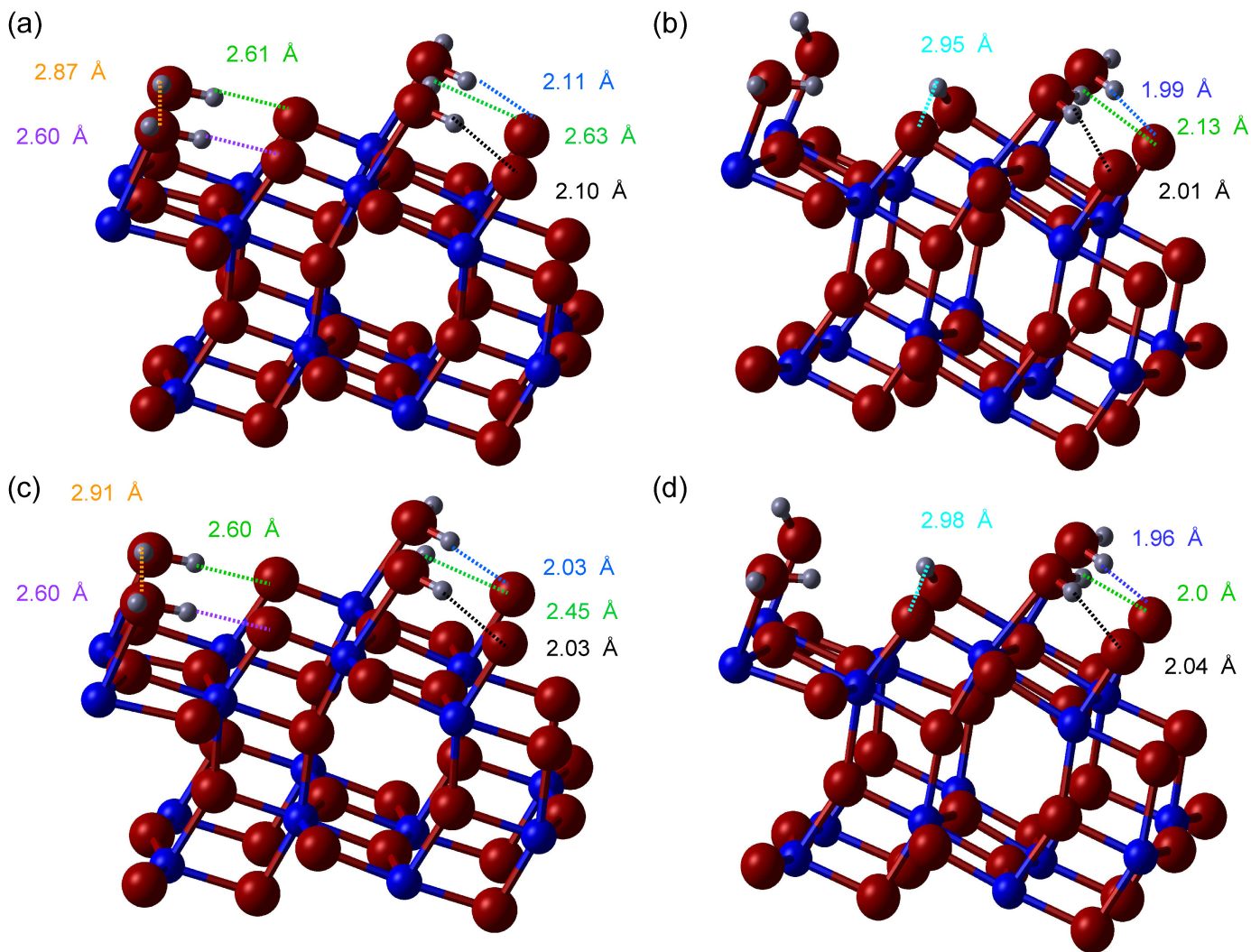


Figure 6: (Color online) Optimised structures and hydrogen bonds resulting from the adsorption of water on anatase (101) at full monolayer coverage and the cases: (a) HSE-molecular, (b) HSE-mixed, (c) PBE-molecular, and (d) PBE-mixed. O2-H distance is shown with dashed lines.

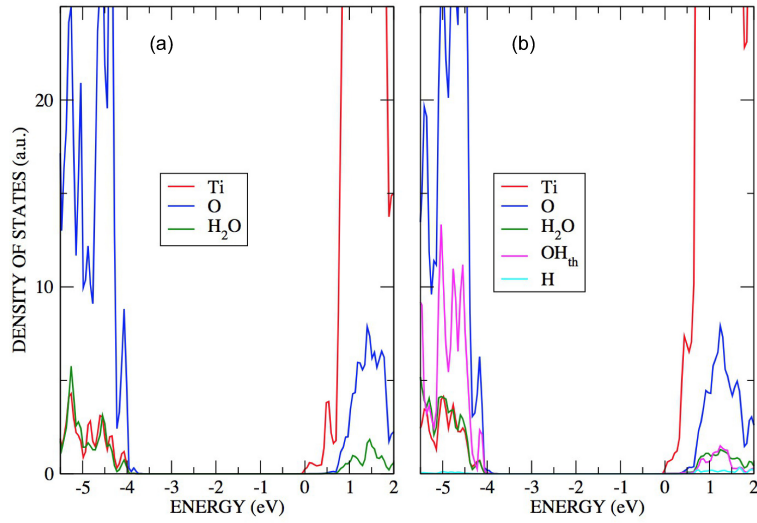


Figure 7: (Color online) DOS for anatase (101) at full monolayer coverage projected on the eight outermost Ti_{5c} and O_{2c} atoms plus water and using the HSE functional for the cases: (a) molecular adsorption of water, and (b) mixed adsorption of water.